Multifunctional carbon foam with hollow-microspheres and concave-convex microstructure for adjustable electromagnetic wave absorption and wearable applications

Yingying He[a], Peiying Xie[a], Shuai Li[a], Yanan Wang[a], Daogui Liao[a], Hongxia Liu[*a], Li Zhou[a], Yunhua Chen[*b]

[a] Guangxi Key Laboratory of Optical and Electronic Materials and Devices, and School of Material Science and Engineering, College of Material Science & Engineering, Guilin University of Technology, Guilin 541004, China

[b] School of Materials Science and Engineering, South China University of Technology, Guangzhou 510640, China

*Corresponding author

Tel: +86-773-5896438

Fax: +86-773-5896211

E-mail: hliu28551@gmail.com (Liu); yhchen0723@gmail.com (Chen)

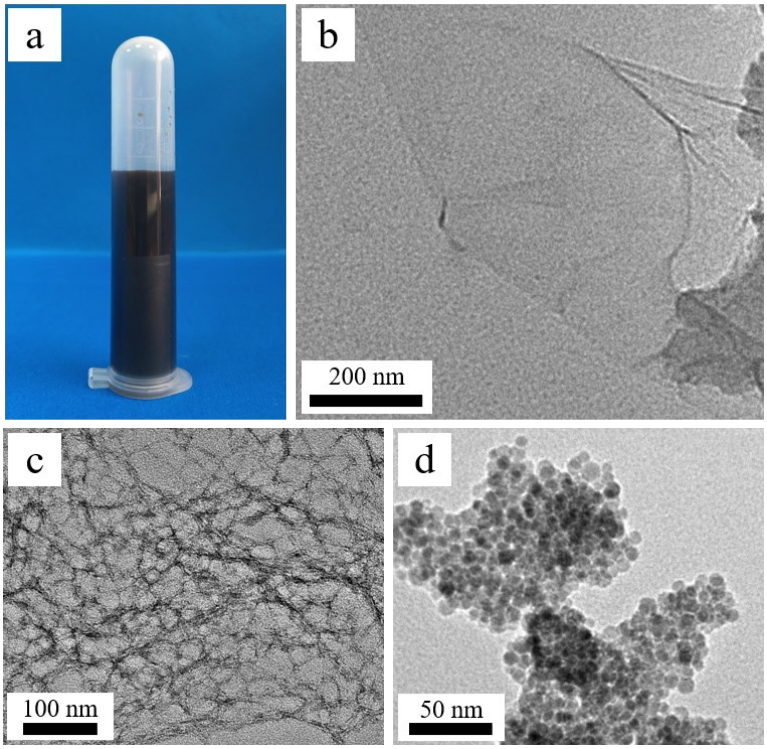

Fig. S1 (a) Digital photo of GO aqueous dispersion, (b) TEM images of GO, CNF and Fe_3O_4 nanoparticles.

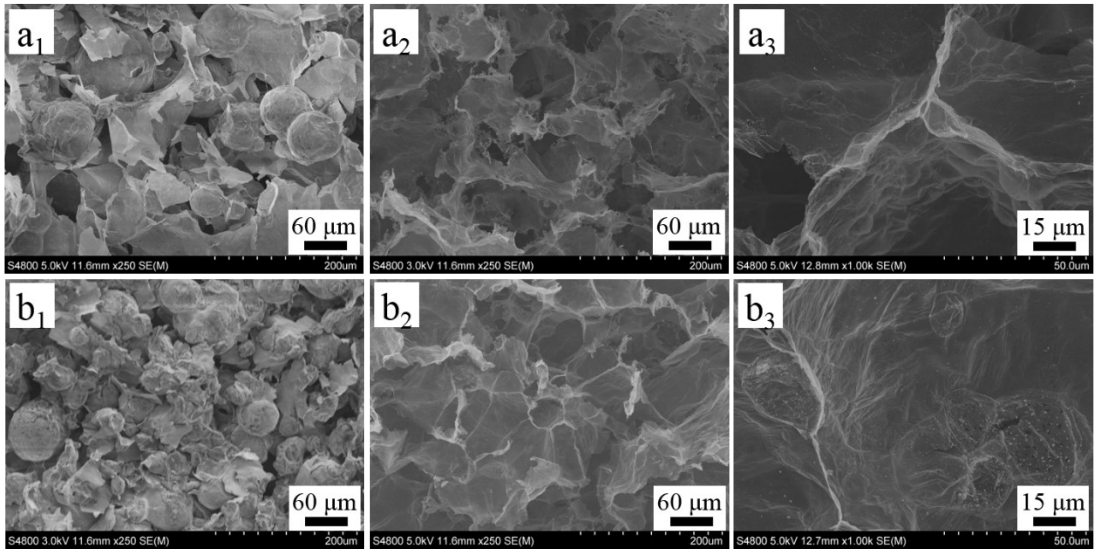

Fig. S2. SEM images of CNF/GO/PW-30/Fe_3O_4-1.0 composite foams obtained at water-oil volume ratios of (a_1) 5:1 and (b_1) 7:1 before carbonization and after carbonization ($a_{2\text{-}3}$, $b_{2\text{-}3}$).

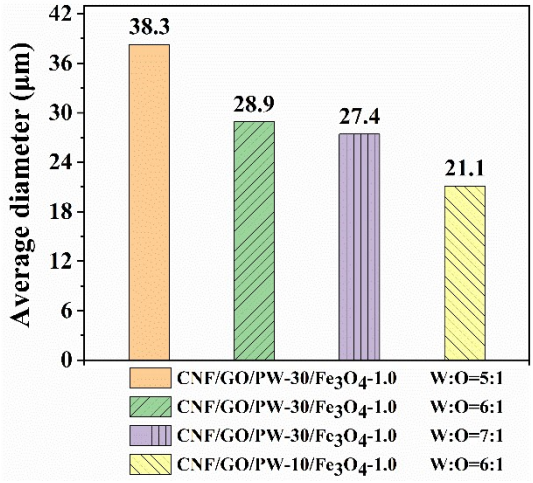

Fig. S3. The corresponding statistical graph of the average diameter of the PW microspheres in the composite foams.

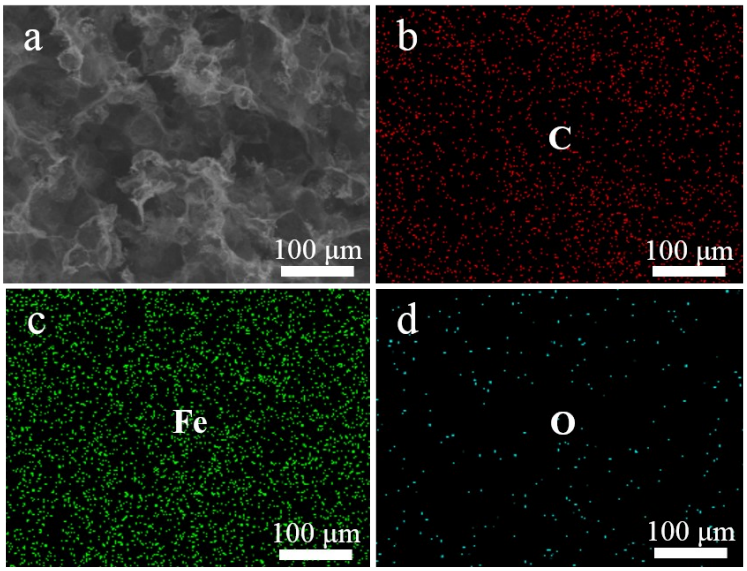

Fig. S4. SEM-mapping pattern of the (a) C-rGO/Fe_3O_4-1.0 carbon foam: (b) C element, (c) Fe element and (d) O element.

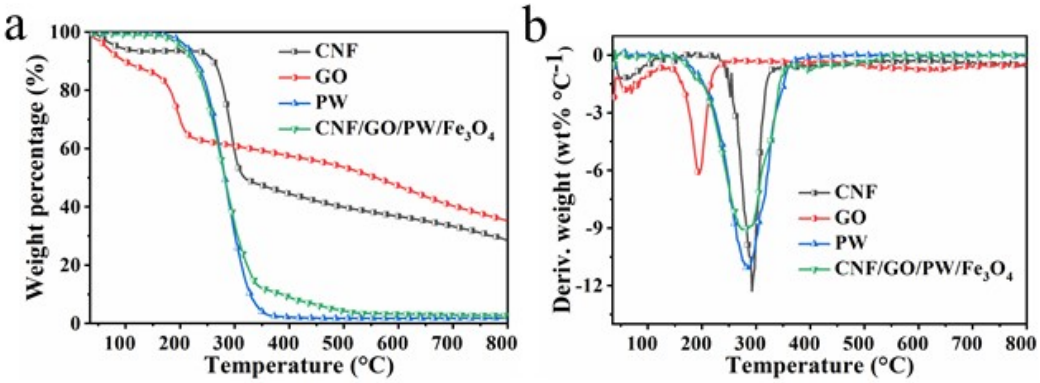

Fig. S5. (a) TG and (b) DTG curve of CNF, GO, PW and CNF/GO/PW-30/Fe_3O_4-2.0 composite foam.

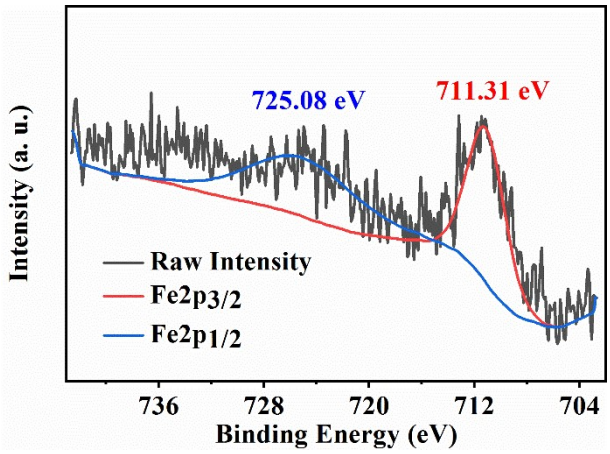

Fig. S6. XPS spectrum of Fe2p of C-rGO/Fe_3O_4-2.5 carbon foam.

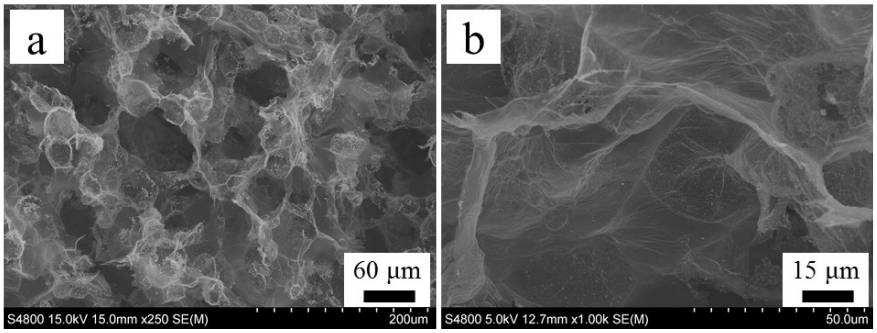

Fig. S7. Different magnification times SEM photos of C-rGO/Fe_3O_4-2.5 carbon foam after 1000 time cycled compression at 60% strain.

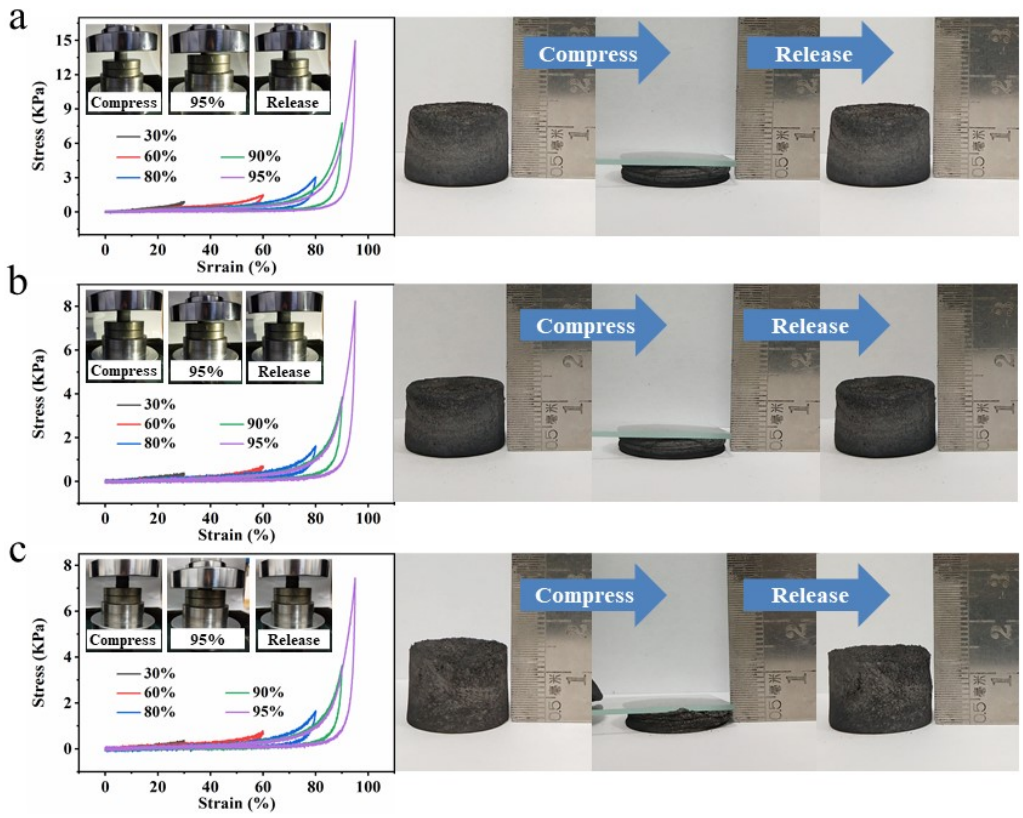

Fig. S8. Stress-strain curves (left) and digital photos (right) of (a) C-rGO/Fe_3O_4-1.0, (b) C-rGO/Fe_3O_4-2.0, and (c) C-rGO/Fe_3O_4-2.5 carbon foams.

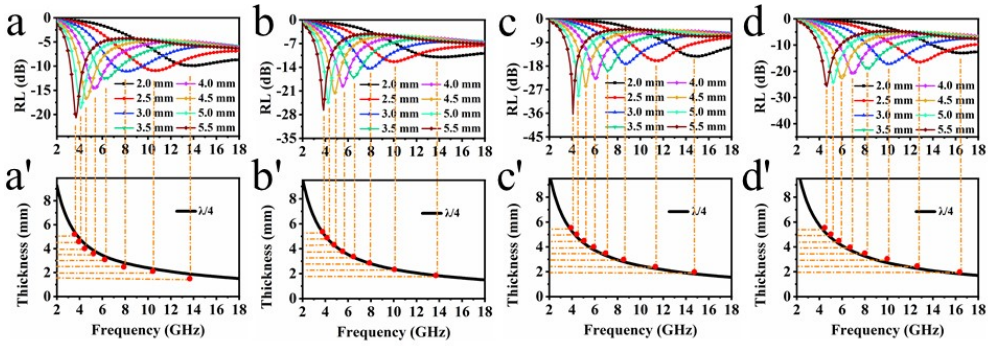

Fig. S9. Simulation of absorber thickness versus peak frequency for (a) C-rGO/Fe_3O_4-1.0, (b) C-rGO/Fe_3O_4-2.0, (c) C-rGO/Fe_3O_4-2.5 and (d) C-rGO/Fe_3O_4-3.0 carbon foams.

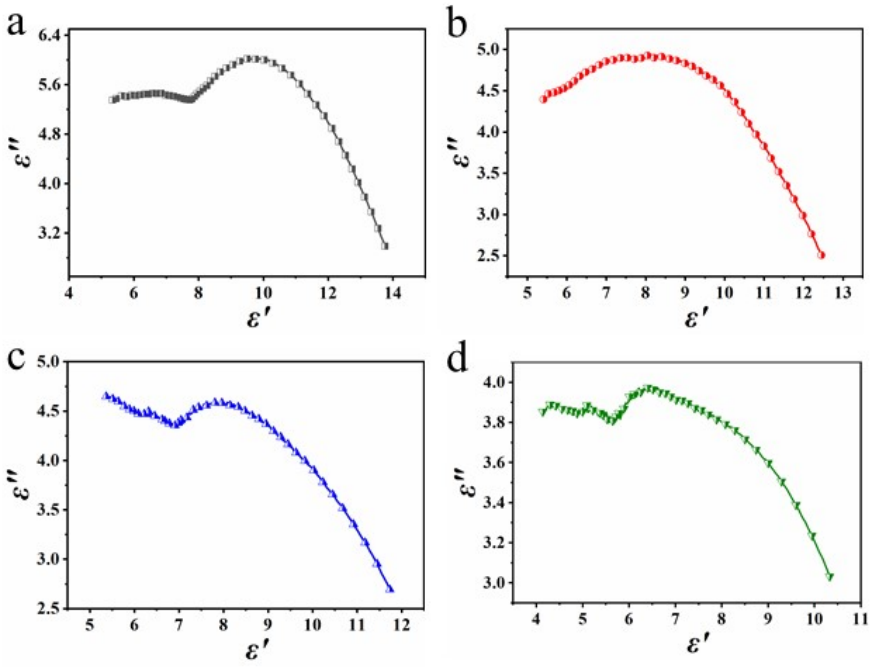

Fig. S10. Dielectric Cole-Cole semicircles of (a) C-rGO/Fe_3O_4-1.0, (b) C-rGO/Fe_3O_4-2.0, (c) C-rGO/Fe_3O_4-2.5 and (d) C-rGO/Fe_3O_4-3.0 carbon foams.

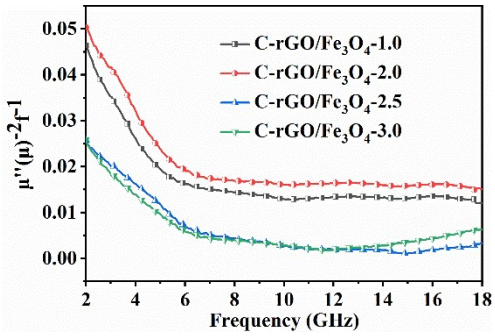

Fig. S11. Frequency dependence of $\mu''(\mu')^{-1}f^{-1}$ values for the carbon foams.

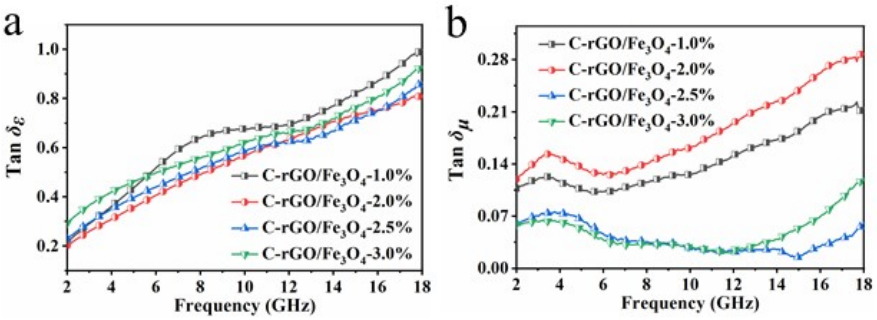

Fig. S12. (a) Dielectric loss tangent and (b) magnetic loss tangent of C-rGO/Fe_3O_4 carbon foams.

Table S1. Experimental recipes of preparing Pickering emulsion gels stabilized by CNFs.

Sample	aqueous : oil（V/V）	PW concentraction (wt%)	Fe_3O_4 concentraction (wt%)
CNF/GO/PW-30/Fe_3O_4-1.0	5:1	30	1.0
CNF/GO/PW-30/Fe_3O_4-1.0	6:1	30	1.0
CNF/GO/PW-30/Fe_3O_4-1.0	7:1	30	1.0
CNF/GO/PW-10/Fe_3O_4-1.0	6:1	10	1.0
CNF/GO/PW-30/Fe_3O_4-0.5	6:1	30	0.5
CNF/GO/PW-30/Fe_3O_4-2.0	6:1	30	2.0
CNF/GO/PW-30/Fe_3O_4-2.5	6:1	30	2.5
CNF/GO/PW-30/Fe_3O_4-3.0	6:1	30	3.0

[a] The density of PW is 0.9 g/cm^3.

Table S2. Electromagnetic wave absorption properties of carbon-based absorbers in this work and the other previous literatures.

Absorbers	RL_{min} (dB)	Thickness (mm)	Effective bandwidth (GHz)	Ref.
$Ti_3C_2T_x$MXene@GO	−49.10	1.2	2.9	1
CeO_{2-x}/rGO	−50.60	1.5	5.8	2
Nitrogen-doped rGO aerogels	−56.40	2.0	6.8	3
NiAl-layered hydroxide/rGO	−41.50	1.4	4.4	4
Graphene aerogel spheres	−52.70	2.3	7.0	5
C@MoO_2/rGO	−35.40	1.5	4.7	6
$CoFe_2O_4$/N-rGO	−55.43	2.3	7.2	7
rGO/PANI	−48.00	2.5	6.0	8
N/B-rGO	−52.00	2.8	6.0	9
CoNi@NC/NCNT/N-rGO	−43.48	3.0	4.2	10
FeNi@NC/NCNT/N-rGO	−39.39	2.0	4.4	11
Ni/MXene/RGO aerogel	−75.2	2.1	7.3	12
CN-REOs	−58.24	1.8	4.8	13
rGO/Ni hybrids	−39.03	2.0	4.3	14
Air@Co@Co_3Sn_2@SnO_2/RGO	−55.49	2.1	5.43	15
C-rGO/Fe_3O_4 carbon foam	−57.50	3.0	6.7	This Work

References

1. Y. Li, F. B. Meng, Y. Mei, H. G. Wang, Y. F. Guo, Y. Wang, F. X. Peng, F. Huang and Z. W. Zhou, *Chemical Engineering Journal*, 2020, **391**.
2. Q. Q. Li, Y. H. Zhao, X. H. Li, L. Wang, X. Li, J. Zhang and R. C. Che, *Small*, 2020, **16**.
3. R. Shu, G. Zhang, C. Zhang, Y. Wu and J. Zhang, *Advanced Electronic Materials*, 2021, **7**.

4. X. F. Xu, S. H. Shi, Y. L. Tang, G. Z. Wang, M. F. Zhou, G. Q. Zhao, X. C. Zhou, S. W. Lin and F. B. Meng, *Advanced Science*, 2021, **8**.
5. T. Li, D. D. Zhi, Y. Chen, B. Li, Z. W. Zhou and F. B. Meng, *Nano Research*, 2020, **13**, 477-484.
6. C. Wu, Z. F. Chen, M. M. Wang, X. Cao, Y. Zhang, P. Song, T. Y. Zhang, X. L. Ye, Y. Yang, W. H. Gu, J. D. Zhou and Y. Z. Huang, *Small*, 2020, **16**.
7. X. Wang, J. Liao, R. Du, G. Wang, N. Tsidaeva and W. Wang, *Journal of Colloid and Interface Science*, 2021, **590**, 186-198.
8. L. Zhang, Z. Zhang, Y. Lv, X. Chen, Z. Wu, Y. He and Y. Zou, *Acs Applied Nano Materials*, 2020, **3**, 5978-5986.
9. Z. H. Sun, Z. Q. Yan, K. C. Yue, A. R. Li and L. Qian, *Composites Part B-Engineering*, 2020, **196**.
10. J. Xu, Y. A. Shi, X. C. Zhang, H. R. Yuan, B. Li, C. L. Zhu, X. T. Zhang and Y. J. Chen, *Journal of Materials Chemistry C*, 2020, **8**, 7847-7857.
11. J. Xu, X. Zhang, H. R. Yuan, S. Zhang, C. L. Zhu, X. T. Zhang and Y. J. Chen, *Carbon*, 2020, **159**, 357-365.
12. L. Y. Liang, Q. M. Li, X. Yan, Y. Z. Feng, Y. M. Wang, H. B. Zhang, X. P. Zhou, C. T. Liu, C. Y. Shen and X. L. Xie, *Acs Nano*, 2021, **15**, 6622-6632.
13. S. Gao, G. S. Wang, L. Guo and S. H. Yu, *Small*, 2020, **16**, 13.
14. W. Xu, G. S. Wang and P. G. Yin, *Carbon*, 2018, **139**, 759-767.
15. G. S. Wen, X. C. Zhao, Y. Liu, D. Z. Yan and Z. Z. Hou, *Chem. Eng. J.*, 2021, **420**, 9.